NOA1 is an essential GTPase required for mitochondrial protein synthesis.

Running Head:

Targeted inactivation of *Noa1* gene in mouse.

Mateusz Kolanczyk[1,2,§,*], Markus Pech[3,*], Tomasz Zemojtel[4,§], Hiroshi Yamamoto[3], Ivan Mikula[5], Maria-Antonietta Calvaruso[6], Mariël van den Brand[6], Ricarda Richter[7], Bjoern Fischer[1,2], Anita Ritz[1,2], Nadine Kossler[1,2], Boris Thurisch[1,2], Ralf Spoerle[8], Jan Smeitink[6], Uwe Kornak[1,2], Danny Chan[9], Martin Vingron[4], Pavel Martasek[5], Robert N. Lightowlers[7], Leo Nijtmans[6], Markus Schuelke[10], Knud H. Nierhaus[3], Stefan Mundlos[1,2] .

[1]Max Planck Institute for Molecular Genetics, Development & Disease Group, 14195 Berlin, Germany

[2]Institute for Medical Genetics, Charitè, Universitätsmedizin, 13353 Berlin, Germany

[3]Max Planck Institute for Molecular Genetics, AG Ribosomen, 14195 Berlin, Germany

[4]Max Planck Institute for Molecular Genetics, Department of Computational Molecular Biology, 14195 Berlin, Germany

[5]Department of Pediatrics and Center for Applied Genomics, Ist Faculty of Medicine, Charles University, 12109 Prague, Czech Republic.

[6]Nijmegen Centre for Mitochondrial Disorders at the Department of Pediatrics, Radboud University Nijmegen Medical Centre, PO Box 9101, 6500 HB, Nijmegen, Netherlands.

[7]Mitochondrial Research Group, Institute for Ageing and Health, Newcastle University, Framlington Place, Newcastle upon Tyne, UK NE2 4HH

[8]Max Planck Institute for Molecular Genetics, Department of Developmental Genetics, 14195 Berlin, Germany

[9]Department of Biochemistry, the University of Hong Kong, Hong Kong, China

[10]Department of Neuropediatrics and NeuroCure Clinical Research Center, Charité University Medical Center, 13353 Berlin, Germany

[§]corresponding authors

kolanshy@molgen.mpg.de; zemojtel@molgen.mpg.de

Max Planck Institute for Molecular Genetics
Ihnestrasse 73, 14195 Berlin
Germany
Fax +49 30 8413 1643
Tel +49 30 8413 1385

Keywords: YqeH, atNOS1, NOA1, hNOA1, ribosome, mitochondria, mitochondrial, ribosome assembly, GTPase, evolution, development, embryogenesis

Abstract

NOA1 is an evolutionarily conserved GTP binding protein, which localizes predominantly to mitochondria in mammalian cells. Based on bioinformatic analysis we predicted its possible involvement in ribosomal biogenesis, although, this had not been supported by any experimental evidence. Here we determine NOA1 function through generation of knock-out mice and in-vitro assays. NOA1 deficient mice exhibit mid-gestation lethality associated with a severe developmental defect of the embryo and trophoblast. Primary embryonic fibroblasts isolated from NOA1 knock-out embryos show deficient mitochondrial protein synthesis and a global defect of oxidative phosphorylation (OXPHOS). Additionally, *Noa1-/-* cells are impaired in staurosporine induced apoptosis. The analysis of mitochondrial ribosomal subunits from *Noa1-/-* cells by sucrose gradient centrifugation and Western blotting showed anomalous sedimentation, consistent with a defect in mitochondrial ribosome assembly. Further, in vitro experiments revealed that intrinsic NOA1 GTPase activity was stimulated by bacterial ribosomal constituents. Taken together, our data show that NOA1 is required for mitochondrial protein synthesis, likely due to its yet unidentified role in mitoribosomal biogenesis. Thus, NOA1 is required for such basal mitochondrial functions as ATP synthesis and apoptosis.

Introduction

Mitochondria are the principal energy produci organelles believed to have evolved from eubacteria that were engulfed by primordial eukaryotic cells (Gray *et al.*, 2001). In the course of evolution mitochondria retained rudimentary genomes, while most of the other necessary genetic information was relocated to the nucleus of the host cell. As a result, in mammalian

cells only 13 proteins are encoded by mtDNA, all of which are translated by mitochondrial and not cytosolic ribosomes. Mitochondrial ribosomes (mitoribosomes) are assembled from more than 70 nuclearly encoded proteins (at least 29 in the 28S small subunit and 48 in the 39S large subunit) and 2 species of mitochondrially encoded rRNA (Koc *et al.*, 2001). Relatively little is known about how these multiple components assemble into a catalytically active complex, and what factors are required for completion of this process. We identified NOA1 (Nitric Oxide Associated-1) as a predominantly mitochondrialy-localized GTP binding protein, homologous to the essential *Bacillus subtilis* GTPase, YqeH (Zemojtel *et al.*, 2006b). YqeH defines a subfamily of circularly permuted GTPases conserved in some species of bacteria and all known eukaryotic organisms (Leipe *et al.*, 2002). The protein belongs to a larger family of YlqF/YawG TRAFAC (translation factors), whose members like YlqF have been implicated in ribosomal assembly in *Bacillus subtilis* (Kim do *et al.*, 2008). Independently of homology to bacterial YqeH, a possible involvement of NOA1 in mitoribosome function has been implicated by data from the yeast protein interactome (Zemojtel *et al.*, 2006a). Here the NOA1 yeast homolog YOR205C was shown to be a part of a protein complex associated with the S5 protein of the small mitoribosomal subunit. YqeH has been suggested to participate in the biogenesis of the 30S ribosomal subunit and to assist in 50S ribosomal subunit assembly (Loh *et al.*, 2007; Uicker *et al.*, 2007). In a recent study human NOA1 was shown to interact with complex I of the electron transport chain and with three mitoribosomal proteins, MRPL12, MRPS27 and MRPS29 (also known as DAP3; death-associated protein 3), indicating NOA1 may interact with the mitoribosome (Tang *et al.*, 2009). To date, however, no experimental data were available to support a role for NOA1 in mitochondrial protein synthesis. Similarly, a physiological role of the protein in mammalian development was also unknown. Here we present a comprehensive analysis of the cellular and developmental role of mammalian NOA1. We show that, NOA1 inactivation impairs mitochondrial protein synthesis, causes global defect of oxidative phosphorylation (OXPHOS), defective apoptosis and mid-gestation lethality of the knock-out mice.

Results

Noa1 gene inactivation results in mid-gestation lethality

In order to experimentally address the function of NOA1 in a physiological *in vivo* context we generated mice in which *Noa1* was inactivated (Figure 1). **M**utant embryos appeared growth retarded and at E9.5 a maximum of 9 somites was observed (Figure 1E-G, Figure 2A). At

E10.5 many embryos were necrotic and no viable *Noa1-/-* embryos were detected thereafter indicating mid-gestation lethality (Table 1). Cell proliferation as measured by BrdU incorporation was drastically reduced in E9.5 *Noa1-/-* embryos (Figure 2A) and very few areas of apoptotic cell death were observed (Figure 2B, C) indicating that cell proliferation as well as apoptosis was severely impaired. Transmission electron microscopy (TEM) of *Noa1-/-* embryos revealed abnormal mitochondria with characteristically swollen cristae (Figure 2D) but no abnormalities in other organelles. In addition, we observed severe defects of the placenta with a reduction of all three trophoblast layers including the trophoblast giant cell layer (TGC) (Figure 3, Supplemental Figure 1). This was in line with *Noa1* being expressed in the trophoblast, but not in the maternal part of placenta (Figure 3A). Together these results indicated that *Noa1* is indispensable for normal development of the embryo and the placenta possibly due to an important function in mitochondria.

Global OXPHOS defect in the Noa1-/- cells.

To gain further information on the biochemical consequences of *Noa1* inactivation we isolated primary embryonic fibroblasts from E9.5 *Noa1-/-* embryos. *Noa1* deficient cells grew in a medium known to compensate for mitochondrial respiratory deficiency and showed no overt abnormalities in the mitochondrial network (Supplemental Figure 3A). To test mitochondrial function we measured cellular respiration by polarographic assays in digitonin permeabilized cells. Complex I, III and IV dependent oxygen consumption was severely reduced in mutant cells (Figure 4A) indicating a global OXPHOS defect. Consequently, *Noa1* knock-out cells showed reduced viability and cellular ATP content when grown under nutrient restriction (Figure 4B, C). Similar results were obtained after *NOA1* depletion in HeLa cells (Supplemental Figure 2).

Since the results of polarographic measurements are influenced by mitochondrial substrate import we further addressed OXPHOS complex function in direct biochemical assays. Spectroscopic assays revealed that the activity of complexes I, III, IV and V were strongly reduced in *Noa1-/-* cells, while the activity of complex II was increased (Figure 4D). Blue-native electrophoresis of isolated mitochondria showed a decreased amount of assembled Complex I, III, IV and V (Figure 4E) and an accumulation of the unassembled complex V (F1) while no free F1 subunit was detected in wild type cells. Confirmatory to this, in-gel activity of complex-I measured by the colorimetric enzymatic assay (IGE) was also strongly reduced (Figure 4E – upper stripe). These findings were suggestive of a general defect of mitochondrial protein synthesis in *Noa1-/-* cells, as complex I, III, IV and V all include

proteins encoded by the mitochondrial DNA whereas all proteins of complex II are encoded in the nucleus and imported into the mitochondrium.

Compromised mitochondrial protein synthesis in Noa1-/- cells

To test this possibility, *Noa1-/-* cells were assayed for mitochondrial protein synthesis. Radioactive methionine labeling showed a deficiency in *de novo* mitochondrial protein synthesis (Figure 5A). Normal copy number and integrity of mtDNA were confirmed by qPCR and long range PCR, excluding defects of replication and/or mtDNA repair as a cause of compromised protein synthesis (Supplemental Figure 3B, C). Expression of genes encoding proteins of the electron transport chain or mitoribosomal function was increased in the mutant cells, indicating that mtDNA transcription in the knock-out cells was maintained, increased expression likely being compensatory to the protein synthesis defect (Figure 5B). Interestingly, 16S rRNA transcript level from the large ribosomal subunit was increased twofold in mutant cells while 12S rRNA remained at the control level indicative of a possible defect of mitoribosome biogenesis (Uicker *et al.*, 2007). These results are consistent with NOA1 being required for mitochondrial protein synthesis.

Altered mitoribosomal profile in the Noa1-/- cells

Protein synthesis within mitochondria is performed by 55S mitochondrial ribosomes (mitoribosomes) which consist of a small 28S subunit and a large 39S subunit. To determine whether the observed mitochondrial protein synthesis defect was due to a ribosomal dysfunction, we compared the mitoribosome sucrose density profiles of wt or rescued cells and those lacking *Noa1*. The small subunit was traced with antibodies against the mitochondrial protein S18b (MRPS18b), which consistently revealed a similar profile between wt (NOA1+/+) and knock-out cells (NOA1-/-). Similar levels of the 28S small subunit were found in fractions 4/5, in the wt, knock-out (NOA1-/-) and complemented cells (NOA1-/- Comp.) but no 55S ribosomes could be visualized (Figure 5C, fractions 8-10). Antibodies against the mitochondrial protein L12 (MRPL12) which reacted with the large 39S subunit (fractions 6 and 7) revealed the decrease in 55S ribosomes in the NOA1-/- cell line (fractions 8-10). Further, although *Noa1* deficiency had only a minimal effect on the position or band intensity of small subunit in the sucrose gradient (Figure 4C, lower panels), the large subunits showed a marked shift to the slower migrating particles (lane 5, NOA1-/- *cf.* NOA1+/+); these effects were rescued by adding *Noa1* in trans (NOA1-/- comp. in Figure 5C). Additionally, NOA1 complementation led to increased abundance of L12 protein in the

fractions 9 and 10. In line with the observed partial rescue of mitoribosomal assembly, retroviral complementation resulted in re-activation of mitochondrial protein synthesis, normalization of respiratory chain complex assembly and improved viability of the knock-out cells (Supplemental Figure 4). These data strongly suggest that inactivation of *Noa1* resulted in an impaired assembly of the 55S mitoribosome.

The GTPase activities of mammalian NOA1 and its bacterial homologue YqeH are stimulated by ribosomal components from E. coli

To gain further insight into NOA1 function, we purified mammalian NOA1 as well as its bacterial homolog YqeH from *Bacillus subtilis*. Both mitochondrial NOA1 and bacterial YqeH, showed a high and comparably strong intrinsic GTPase activity (Figure 6A). This was not observed with other G-factors involved in translation such as EF-G, which can be stimulated exclusively by 70S ribosomes during protein synthesis and is boosted by empty 70S uncoupled from protein synthesis (Gordon, 1970; Qin *et al.*, 2006). In line with a previously proposed role in 30S assembly, YqeH GTPase activity could be stimulated by *Escherichia coli* 16S rRNA, more than two-fold, whereas the addition of 23S rRNA had no effect (Figure 6B), similar to poly(U) addition (not shown).

In addition, 21S precursor particles of the 30S subunit stimulated the YqeH GTPases activity rather than mature 30S and 50S subunits or 70S ribosomes (Figure 6C). In contrast, NOA1 activity was stimulated by rRNAs of the small and large ribosomal subunits from both mammalian (human) mitochondria (12S and 16S rRNAs) and *Escherichia coli* (16S and 23S rRNAs) by 40% (Figure 6D). Precursor of the 30S *Escherichia coli* ribosome, the 21S particle prepared by total reconstitution (Nierhaus, 1990), stimulated NOA1 activity with about the same intensity (Figure 6E). Total reconstituted 30S particle as well as native 30S subunits induced a striking two-fold increase of GTPase activity. Interestingly, the strongest effect was observed with 50S particles, whereas 70S ribosomes showed four-times less stimulation underlining the specificity of the observed effects. These results suggest an involvement of both bacterial YqeH and mammalian NOA1 in ribosomal biogenesis.

Noa1-/- cells are resistant to staurosporine induced apoptosis

NOA1 was previously reported to be involved in regulation of apoptosis in HeLa cells (Tang *et al.*, 2009). To verify if the mitochondrial defects in NOA1-deficient cells would also be accompanied by the impairment of apoptosis, embryonic fibroblasts were treated with staurosporine and apoptosis was monitored by accumulation of the cleaved caspase-3. A robust caspase-3 activation was detected 24 h post-induction in the control cells but was

entirely absent in the mutant cells (Figure 7). Retroviral reconstitution of NOA1 expression partially restored caspase-3 activation in *Noa1-/-* cells (Supplemental Figure 4E). Additionally, mitochondrial membrane potential determined with JC1 staining was increased in knock-out cells corroborating the observed apoptosis defect (Supplemental Figure 4F). Thus, NOA1 is necessary for activation of caspase dependent apoptosis.

Discussion

In the current study we address both, the cellular and the developmental function of NOA1 by inactivating the gene in mice. The vital role of *Noa1* was underlined by a massively restricted growth and arrested proliferation at ~E9.5 followed by death of *Noa1-/-* mice at ~E10.5 (Table 1 and Figure 1, Figure 2A). The mitochondria in these developing embryos showed aberrations of cristea morphology, whereas other organelles appeared not to be affected (Figure 2D). Thus, both the timing of the lethality as well as the results of EM analysis reflect the important mitochondrial function of NOA1. Interestingly, the developmental defect extended to the placental trophoblast which constitutes the interface between maternal and embryonic circulation (Figure 3B, Fig S1) (Red-Horse *et al.*, 2004). The defect occurs at relatively early stage of trophoblast differentiation as revealed by the diminished expression of 4311/Tbpb, demarcating population of trophoblast progenitor cells at E8.5. The dependence of trophoblast development on NOA1 function exposes a crucial role of mitochondria in the development of the maternal-fetal interface. The importance of mitochondrial function in this process is further supported by the observation that knock-outs of mitochondrial fusion factor Mtf2 as well as this of mito-division factor Drp1 result in a deficiency of trophoblast giant cells (Chen *et al.*, 2003; Wakabayashi *et al.*, 2009).

The nature of NOA1 mitochondrial function was investigated in the primary knock-out mouse embryonic fibroblast cells. *Noa1-/-* cells were shown to have impaired activities of the electron transfer chain complexes I, III, IV and V but not of complex II, which lends strong support to NOA1 being required for expression of the mitochondrial genome. We therefore analysed all stages of mtDNA expression and determined that NOA1 deficiency impairs protein synthesis but does not cause loss of mtDNA and/or transcription. Thus, NOA1 appears specifically required for mitochondrial protein synthesis. Sucrose gradient centrifugation and Western blot experiments revealed that knock-out cells exhibit an aberrant migration of the large mitoribosomal subunit, indicating NOA1 is required for correct mitoribosome assembly (Figure 5D). However, involvement of NOA1 in the biogenesis of the small mitoribosomal

subunit cannot be ruled out at present. In this study, our choice of antibodies against mouse small mitoribosomal subunit was limited to anti-MRPS18b, which did not show any defect. Several other commercially available anti-MRP antibodies were tested but none were capable of cross reactivity with murine MRPs (data not shown).

Our knowledge about mitochondrial ribosome biogenesis and function is essentially based on the studies of bacterial and yeast model systems. Ribosome assembly comprises the processing and folding of pre-RNA and its concomitant assembly with ribosomal proteins. A large number of ribosomal constituents as well as non-ribosomal factors are involved. Among these factors the GTPases, a family of energy consuming enzymes characterized by the so-called G-domain, have been shown to play key roles in the assembly of ribosomes in bacteria (Karbstein, 2007; Britton, 2009). As shown here, mitochondrial NOA1, similarly to its bacterial homologue YqeH, has GTPase activity. The intrinsic GTPase activity of the *Bacillus subtilis* YqeH, is strongly and specifically stimulated by 16S rRNA of the small subunit from *Escherichia coli* as well as by the 21S reconstitution intermediate of the small subunit, which is highly similar to the native 21S precursor particle - for review see (Nierhaus, 1991). The strong stimulation contrasts with the effects of 23S rRNA and the mature ribosomal subunits, which did not stimulate the intrinsic activity of YqeH. This finding supports the notion that the major activity of the bacterial YqeH is related to the early assembly phase of the small subunit. Interestingly, this was different for mammalian NOA1, which was stimulated both by the bacterial 50S large ribosomal subunit as well as by 30S small subunit. To a lesser degree, NOA1 was also stimulated by naked rRNAs, and precursor 21S particles, whereas only residual stimulation was observed with full 70S ribosomes. This data show that NOA1 like its bacterial homologue YqeH has GTPase activity, which is stimulated by the bacterial ribosomal constituents. The apparent difference in NOA1 and YqeH specificity likely reflects their evolutionarily divergence. Indeed, NOA1 contains ~100 aminoacid insertion in the GTP binding domain which is absent from bacterial YqeH and *Arabidopsis* NOA1 proteins and this could explain the differences in protein target recognition (Zemojtel *et al.*, 2004). Together with the observed aberrant migration of the large ribosomal subunit in the *Noa1* knock-out cells this further suggests a possible involvement in the mitoribosome biogenesis.

Several proteins involved in mitochondrial protein synthesis have been shown to be involved in the process of apoptosis. Among them were mitoribosomal GTP binding protein MRPS29/DAP-3 (Death Associated Protein-3), MRPS30/PDCD9 or p52 (programmed cell death protein 9) and a protein with an apparent dual cell protective as well as pro-apoptotic function PDCD8/AIF – (Apoptosis Inducing Factor) (Cavdar Koc *et al.*, 2001; O'Brien, 2002;

Cheung *et al.*, 2006). Interestingly, DAP3 was among several ribosomal proteins recently shown to interact with NOA1 (Tang *et al.*, 2009).

Similarly to DAP3, NOA1 appears to be necessary for mitochondria dependent apoptosis. The primary fibroblasts isolated from the knock-out embryos were impaired in staurosporine induced apoptosis (Figure 7A) and retroviral complementation partially reversed this phenotype (Supplemental Figure 4E). Importantly, NOA1 inactivation results in hyperpolarization of mitochondria, which likely contributes to the phenotype of defective apoptosis (Supplemental Figure 4F). In line with that, NOA1 knock-down in neuroblastoma cells was reported to result in mitochondrial hyperpolarization, preventing cytochrome-c release (Parihar *et al.*, 2008). Thus, while exact molecular mechanism remains yet to be discovered, it is increasingly clear that a group of mitoribosome associated proteins, including NOA1, is required for the execution of programmed cell death.

Interestingly, NOA1 appears to play a similar role in plants, as *Arabidopsis* NOA1 (formerly atNOS1 – Nitric Oxide Synthase 1) was shown to localize to plastids, where it is necessary for protein synthesis (Flores-Perez *et al.*, 2008). Similarly, plastidial NOA1 localization was shown in the phytoplankton Diatom - *Phaeodactylum tricornutum* (Vardi *et al.*, 2008). Remarkably, deficient growth and greening phenotype of atNOA1 deficient plants could be complemented by *Bacillus subtilis* YqeH fused to the *Arabidopsis* NOA1 organelle localization sequence (Flores-Perez *et al.*, 2008), clearly demonstrating that YqeH is a functional orthologue of plastid localising atNOA1. Like mitochondria, plastids are believed to have originated from eubacterial endosymbionts. Thus mammalian NOA1 is an evolutionarily extremely conserved GTPase, required for protein synthesis in both procaryota-derived organelles. Further investigation into NOA1 structure and function is needed to unravel the exact mechanisms of its function in relation to mitoribosome and apoptotic action. The *Noa1* inactivation in mouse however, demonstrates that this gene product plays a vital role in mitochondrial homeostasis and mammalian development.

Materials and Methods

Tissue isolation and processing

Pregnant mice were intraperitoneally injected with BrdU solution (10 µl of 10 mM solution / 1 g of mouse body weight) 1 h before sacrifice. Embryos were dissected from deciduas using an inverted microscope (Leica, Germany). Whole embryos were photographed in PBS using a microscope mounted digital camera (Leica, Germany). Embryonic stages were estimated by

timed pregnancies and somite counts. The embryos were fixed in 4% PFA pH 7.4, dehydrated in ethanol, and paraffin embedded. The specimens were sectioned at 6 µm, stained with hematoxilin-eosin or processed for immunohistochemical staining.

Mouse embryonic fibroblast (MEFs) culture.

Eviscerated embryos were collected in u-well bottomed 96 well plates, cut into small fragments with dissection forceps and digested in 25 µl cell culture grade 0.5% w/v trypsin at 37°C for 20 min. Subsequently they were dispersed by pipeting and plated into 1 well of the 96 well flat bottomed plate in 200 µl of fresh DMEM containing 1 g/l glucose, 10% FBS, 2% penicillin/streptomycin, 50 µg/ml l-uridine (Sigma), 0.1 mM nonessential amino acids (Invitrogen), 1 mM sodium pyruvate (Sigma), 10% Amniomax C-100 supplement (Invitrogen). The media was changed every second day until cells reached confluence. Cells were subsequently expanded and continuously passaged until spontaneously immortalized colonies were derived. Cells were cultured at 37°C in 95% air / 5% CO_2.

Retroviral infection.

BOSC23 packaging cells were transiently transfected with a retroviral vector expressing mouse *Noa1* (pQCXIP-mNOA1) using the CalPhos™ Mammalian Transfection Kit (Clontech). Retroviral stocks were collected 48h post transfection. *Noa1* deficient MEFs were infected with the retrovirus in the presence of 6 µg polybrene and selected for 4 days with 2,5 µg/ml puromycin.

Immunofluorescence

For BrdU detection sections were pre-treated by 2N HCl treatment and incubated with a monoclonal antibody against BrdU (1:50; Roche). Apoptotic cell death was visualized in the whole mount specimens with antibodies against activated caspase-3 (Cell Signalling). TUNEL assays on the paraffin sections were performed using the in situ cell death detection kit (Roche Diagnostics) following the manufacturer's protocol. Alexa-568 and/or Alexa-488 conjugated goat anti rabbit secondary antibodies were used in all experiments.

Quantification of immunofluorescent staining

Embryonic fibroblasts were seeded on cover slips. After 12 h the cells were treated with increasing concentrations of staurosporine (Sigma). 18 h later cells, cells were processed for immunofluorescence by fixing in 4% paraformaldehyde; 1xPBS for 10 min and

permeabilizing with 0.4% Triton-X100; 3% BSA; 1xPBS for 10 min at 4°C. Incubation with an antibody against activated caspase-3 (Cell-Signalling) 1:400 was performed over night in 3% BSA at 4°C. For visualization, an anti-rabbit IgG Alexa Fluor 488 (Invitrogen, Molecular Probes) conjugate was applied. Nuclei were stained with DAPI and cells were mounted in Fluoromount (Scientific Services). Cells were photographed using a fluorescence microscope (BX60 - Olympus) or scanning microscope (LSM510meta - Zeiss). For each treatment, at least 10 images were evaluated with ImageJ software. Experiments were repeated at least 3 times and more than 1,000 cells per sample were counted.

Immunocytochemistry

Cells grown on gelatin-coated coverslips were fixed with 4% parformaldehyde and permeabilized in PBS/0.1% Triton X-100. Non-specific binding was reduced by blocking with 5% bovine calf serum in PBS and the cells were incubated with primary antibody in 1% BSA/PBS.

In-situ hybridization

Embryos in deciduas were fixed overnight at 4°C in 4% paraformaldehyde, dehydrated through an ethanol and xylene series, and embedded in paraffin blocks. 6-µm sections were cut in a transverse plane with respect to the placenta. Slides were processed for hematoxylin-eosin staining and in-situ hybridization as previously described (Vortkamp *et al.*, 1996). Riboprobe template vectors were kindly provided by Malgorzata Gasperowicz and James Cross, University of Calgary, Canada. For genotyping, embryonic tissue was scraped off unstained slides. DNA was recovered and genotyped by PCR.

HeLa cell culture and siRNA transfections

HeLa human cervical carcinoma cells were maintained in DMEM medium (4,5 g/l glucose) supplemented with 10 % FCS, penicillin G (100 IU/ml), streptomycin (100 g/ml), and l-glutamate (2 mM) and cultured at 37°C in a humidified atmosphere containing 5% CO_2 and 95% air. The sequence of the sense strand of the NOA1 targeting siRNA was (GGUCAUACGUUACUCCAGA) dTdT. siRNA was transfected using 'Dreamfect' (Ozbiosciences). 60% confluent cells were transfected with (1 µM) siRNA (20 nmol dsRNA) according to supplied protocol. Following transfection cells were cultured in DMEM containing 10% FCS for 3 days. 72 h post transfection cells were harvested for analysis. HeLa cells transfected with scrambled siRNA were used as control.

Western Blotting

Protein lysates were prepared in SDS RIPA buffer supplemented with complete proteinase inhibitor tablet (Roche), PMSF (1 mM), sodium vanadate (1 mM) and sodium fluoride (1 mM). The lysate concentrations were determined using Bradford assay (BioRad). Lysates (40 µg of protein per well) were resolved in 10% SDS PAGE and subsequently transferred to PVDF membranes. The blots were probed with the rabbit anti-NOA1 polyclonal antibody generated against peptide: CVNVKGQRMKKSVAYK (1:100). Other antibodies used were: rabbit anti-actin (1:1000) (Sigma). Blots were developed with the ECL+ Lightning system (PerkinElmer).

Transmission Electron Microscopy

Whole E9.5 embryos were fixed with 2.5% glutaraldehyde in 0.1 M cacodylate buffer solution (pH 7.3) at 4°C, washed, and postfixed in 2% osmium tetroxide in the same buffer. Samples were dehydrated in ethanol, then embedded in Eponate 12 epoxy resin (Serva) and sectioned on Reichert-Jung Ultracut microtome. Semi-thin sagittal sections of whole embryos were stained with methylene blue-azure to locate and mark the somite regions. The ultrathin sections were prepared, stained with uranyl acetate, followed by lead citrate, and imaged using EM906 Zeiss electron microscope at 80 kV.

Optical Tomography

OPT method was used to visualize embryos in 3D. The method accumulates projection images of an entire specimen from many different angles, and recalculates the original 3D structure by using a "back-projection" reconstruction algorithm (Sharpe *et al.*, 2002). OPT-scans were performed in UV light using a GFP1 filter for detection of the embryos auto-fluorescence using IPLab software from ScanAnalytics. Results were exported to QuickTime movies.

Polarography

Mouse embryonic fibroblasts (MEFs) and siRNA treated HeLa cells were trypsinized, washed twice with PBS and permeabilized with 50 µg/ml digitonin. The optimum incubation time for permeabilization (50 sec for MEFs; 120 sec for HeLa) was determined in separate time series for each cell line and defined as the shortest duration after which 99% of the cells were trypan-blue positive. Additionally, we verified adequate mitochondrial coupling by

measuring the increase of respiration after decoupling with DNP (2,4-dinitrophenole) in comparison to the state IV respiration without ADP. The DNP / state IV respiration rates were 1.7±0.1 in wildtype cells and 1.8±0.2 in the knock-out MEF cells. The cells (1×10^7) were resuspended in reaction buffer and introduced into the reaction chamber of a Clark-type electrode (Hansatech), and oxygen concentrations were measured in 1 ml volume at 37 °C with substrates and inhibitors according to standard protocols (Hofhaus *et al.*, 1996). After completion of the polarographic measurement, cells were collected and DNA quantified using Quant-iT™ *PicoGreen* DNA kit (Invitrogen) according to the supplied protocol. Oxygen consumption was given as mean ± SD nmol O_2 per minute per µg DNA ($n\geq4$).

Blue-native PAGE and complex I in-gel activity assay

Blue-native PAGE was used for separation of the OXPHOS complexes on 5–15% polyacrylamide-gradient gels as described before (Calvaruso *et al.*, 2008). After electrophoresis of 40 µg protein from mouse embryonic fibroblasts, gels were further processed for in-gel activity assays and western blotting. Assembly of the OXPHOS complexes were analyzed using monoclonal antibodies against subunits of complex I (NDUFA9, NDUFS3), complex III (Core2), Complex V (α-ATPase) (Molecular Probes, Leiden, The Netherlands), Complex II (SDHA) and IV (CoxVa) (MitoSciences, Eugene, OR, USA).

Oxidative phosphorylation enzyme complex measurements

The activities of the OXPHOS enzyme complexes were measured in mouse embryonic fibroblasts as described previously (Lazarov and Cooperstein, 1951; Smeitink *et al.*, 2001; Janssen *et al.*, 2003; Janssen *et al.*, 2007). Citrate synthase (CS) activities were determined in cultured fibroblast as previously described (Srere, 1969).

Analysis of mitochondrial protein synthesis

In vitro pulse labeling of mitochondrial translation products was performed as described elsewhere (Boulet *et al.*, 1992), with a few adaptations. In brief, cells were labeled for 60 min at 37°C in L-methionine-free and L-cysteine-free DMEM with 10% dialyzed FCS, 200 µCi/ml [^{35}S]methionine and [^{35}S]cysteine (Tran35S-Label, MP Biomedicals, Eindhoven, The Netherlands) and 100 µg/ml emetine, and subsequently chased for 10 min in regular DMEM with 10% FCS. Total cellular protein was resuspended and incubated for 10 min in PBS containing 2% laurylmaltoside. Unsolubilized material was removed by centrifugation at

10,000 g for 10 min. The protein concentration was determined (micro BSA protein assay kit, Pierce) and loading buffer was added to the supernatant 1:1 (Tricine Sample Buffer, Bio-Rad). The samples were separated through 16% polyacrylamide gels and subsequently scanned on a FLA5100 (Fujifilm Life Science, Düsseldorf, Germany). Equal protein loading was confirmed using Colloidal Coomassie blue staining (data not shown).

Isokinetic sucrose gradient analysis of mitochondrial ribosomes

Cell lysis was performed in 50 mM Tris-HCl, pH 7.4, 150 mM NaCl, 1 mM EDTA, 1% Triton X-100, + PI-Mix, 1 mM PMSF, 10 mM $MgCl_2$ for 30 min at 4˚C. After 10 min incubation, lysate was clarified by centrifugation at 12,000 g at 4˚C. Approximately 0.9 mg of supernatant was loaded on a linear sucrose gradient (10-30% [v/v], 1 ml) in 50 mM Tris-HCl pH 7.2, 10 mM $Mg(OAc)_2$, 40 mM NH_4Cl, 100 mM KCl, 1 mM PMSF, 50 µg/ml chloramphenicol and centrifuged for 2 h 15 min at 100,000 *g* at 4˚C. Fractions of 100 µl were collected and 10 µl of each fraction was analyzed by Western blot. Antibodies used: anti-MRPS18b (ProteinTech Group, Inc), anti-MRPL12 (Abcam)

Quantitative RT–PCR

cDNAs were synthesized from 1 µg total RNAs with MuLV reverse transcriptase (Applied Biosystems). TaqMan universal PCR was then performed on an ABI PRISMs 7900 cycler (Applied Biosystems), using the SYBR green method according to the manufacturer's instructions. Transcripts of the following genes were monitored: NOA - NOA1, 16S RNA, 12S RNA, ND1 - NADH dehydrogenase subunit 1; ND6 - NADH dehydrogenase subunit 6, CytOx1 - Cyt c oxidase subunit 1, CytOx2 - Cyt c oxidase subunit 2, cytB - cytochrome b, ATP6 - ATP synthase F0 subunit 6, EF-Tu - Elongation Factor Tu, L20 - mitochondrial ribosomal protein L20, AIF - apoptosis inducing factor – see also supplemental primer list.

mtDNA analysis

mtDNA/nDNA ratio was estimated using qPCR with primers specific for mitochondrial DNA encoded *Cox1* gene (subunit I of cytochrome c oxidase) and nuclearly encoded *Ndufv1* gene (NADH:ubiquinone oxidoreductase) (Supplemental Primer List)**.** DNA quantification was repeated five times in independent qPCR reactions and an average mtDNA/nDNA ratio calculated. All values were expressed as means±SD.

Mitochondrial genome integrity was tested using primers listed in supplement and ExpandTM Long Template PCR system (Roche) according to manufacturer's protocol. PCR

conditions were: (94°C 3 min; 10 cycles: 94°C 10 s, 65°C 30 s, 68°C 16 min; 20 cycles: 94°C 10 s, 65°C 30 s, 68°C 16 min (+20 s/cycle). For detection of shorter products, elongation time was reduced to 8 min.

ATP assay

ATP levels were measured with the Bioluminescence Assay Kit - ATPlite (Roche). Cells were trypsinized after 36 h incubation time in culture medium with (4.5 g/l) or without glucose. The cells were washed once in PBS and resuspended in the kit's dilution buffer.

Viability assay

Viability was measured with Alamar Blue assay according to supplied protocol (BioZol). Defined cell numbers were plated in 96 well formats and the resazurin substrate reduction was monitored in the cell culture medium by measuring accumulation of the fluorescent resorufin (excitation at 530 nm, emission at 590 nm).

Preparation of ribosomal RNA

16S rRNA and 23S+5S rRNA of *Escherichia coli* were prepared by phenol extraction followed by ethanol precipitation starting with purified 30S and 50S ribosomal subunits, respectively (Lietzke and Nierhaus, 1988). The genes coding for the mitochondrial 12S and 16S ribosomal RNA were amplified from human mitochondrial DNA using the primers mt12S fw and mt12S rev or mt16S fw and mt16S rev leading to the fusion of a T7 promoter sequence at the 5'-end of the genes. PCR fragments were digested with *Hind*III and *Eco*RI and cloned into pSP65 cleaved with the same enzymes. Transcription of the genes was performed *in vitro* using T7 RiboMAX™ Express (Promega) with the new constructed plasmids (linearized with *Eco*RI) as template. Transcribed RNA was purified by gel filtration and ethanol precipitation.

Cloning, expression and purification of Bacillus subtilis YqeH and human NOA1

The gene coding for *Bacillus subtilis* YqeH was amplified from genomic DNA by PCR and cloned into pET28a (Novagen) *via Nde*I and *Xho*I leading to an N-terminal His-tag fusion. The correct sequence was confirmed by sequencing. The gene was expressed in BL21(DE3) and the protein purified via Ni-NTA agarose (Qiagen, according to the manufactures manual) followed by anion exchange chromatography (MonoQ, GE

Healthcare). The protein was finally dialyzed against 20 mM Hepes•KOH (pH 8.0 at 0 °C), 6 mM $Mg(acetate)_2$, 150 mM K(acetate), 4 mM β-mercaptoethanol.

Full-length cDNAs for human NOA (IRALp962E057Q2) was obtained from the German Resource Center for Genome Research (RZPD). The gene coding for □25a.a.-hNOA1 protein (hNOA1 without mitochondria targeting sequence - 25 amino-acids of N-terminus) was amplified by PCR and cloned into pGEX-6P (Amersham) /via/ *Eco*RI and *Xho*I leading to an N-terminal GST-tag fusion. The gene was expressed in BL21-CodonPlus (DE3)-RP (Stratagene) and the protein purified via Glutathione Sepharose 4B (Amersham) using PBS buffer pH 6.2 supplemented with 1% Triton X-100, according to the manufactures manual. The protein was finally dialyzed against 50 mM Tris pH 7.0 at 4^oC, 150 mM NaCl and concentrated using Centriprep YM-10 (Amicon).

30S reconstitution and poly(Phe) synthesis

0.125 A_{260} of 16S *Escherichia coli* rRNA equivalent to 9 pmol was incubated with 0.05 equivalent units (e.u.) of total proteins of the 30S subunit (TP30) for 30 min at 40°C in 15 ml in Rec20 buffer conditions: 20 mM Hepes-KOH (pH 7.6 at 0°C), 20 mM $Mg(acetate)_2$, 400 mM NH_4(acetate), 4 mM β-mercaptoethanol for details see (Nierhaus, 1990). Subsequently poly(U) dependent poly(Phe) synthesis was performed with 6 pmol of reconstituted particles, which were incubated at 37°C for 1 hour in 40 µl with 6 pmol 50S subunits, 13.4 µg $tRNA^{bulk}$, 33.4 µg poly(U), 10 nmol of phenylalanine (23 dpm/pmol), 3.33 µl S100 enzymes in the presence of 20 mM Hepes-KOH (pH 7.6 at 0°C), 6 mM $Mg(acetate)_2$, 150 mM NH_4(acetate), 4 mM β-mercaptoethanol, 2 mM spermidine, 0.05 mM spermine, 3 mM ATP, 1.5 mM GTP, 5 mM acetyl-phosphate. 35 µl of the reaction mix was subjected to hot TCA precipitation and filtered through glass filters. Control reconstitutions were performed at 20°C for 1 h, but otherwise under identical conditions in the presence and absence of 9 pmol of YqeH. The *Bacillus subtilis* YqeH factor did not accelerate the *Escherichia coli* reconstitution process of the 30S subunit.

Preparation of 21S particle

600 A_{260} of 16S rRNA and 240 e.u. of TP30 were reconstituted for 30 min in ice water. The incubated sample was centrifuged through a 10-30% sucrose gradient containing Rec20 in a Beckman Zonal rotor at 24,000 rpm for 19 hours at 4 °C. Fractions containing the heavy shoulder of the 21S peak were collected and the particles were pelleted, resuspended in Rec20 buffer. Protein content of the 21S particles was determined by 2D electrophoresis, the

following proteins were detected: S4, S5, S7, S8, S9, S13, S14, S15, S16, and S18. The proteins S1 and S20 could not be resolved on the 30S control. The intactness of the rRNA was confirmed by RNA electrophoresis. Controls containing the 21S particles were subjected to a reconstitution incubation in the presence of TP30 and checked for poly(Phe) synthesis in the presence of mature 50S subunits. The results confirmed that the 21S particle were authentic intermediates, which could be processed to active 30S subunits.

GTPase assay

The assay was performed in a 50 µl reaction volume under optimized ion conditions (20 mM Hepes-KOH (pH 8.0 at 0°C), 4.5 mM $Mg(acetate)_2$, 150 mM K(acetate), 2 mM spermidine, 0.05 mM spermine, 4 mM β-mercaptoethanol. The incubation mixture contained 10 pmol YqeH or NOA1, 2.5 nmol [γ^{32}P]GTP (20 dpm/pmol) and the indicated amounts of ribosomal RNA, 21S particles or ribosomal subunits. Samples were incubated either 1 h / 30°C or 6 h / 20°C and the reaction was stopped by addition of 120 µl 0.5 M H_2SO_4, 1.5 mM NaH_2PO_4. The released γ-phosphate was extracted by mixing the samples with 30 µl 200 mM $MoNaO_4$ and 800 µl water-saturated 2-butanol. Samples were vortexed for 1 min followed by centrifugation 16,000 x *g*, 10 min, 4°C. The radioactivity obtained in the buthanol phase was measured in a Wallac 1409 Liquid Scintillation Counter.

All animal experimental procedures were approved by the local animal ethics commission -*LaGeSo*.

References

Boulet, L., Karpati, G., and Shoubridge, E.A. (1992). Distribution and threshold expression of the tRNA(Lys) mutation in skeletal muscle of patients with myoclonic epilepsy and ragged-red fibers (MERRF). Am J Hum Genet *51*, 1187-1200.

Britton, R.A. (2009). Role of GTPases in bacterial ribosome assembly. Annu Rev Microbiol *63*, 155-176.

Calvaruso, M.A., Smeitink, J., and Nijtmans, L. (2008). Electrophoresis techniques to investigate defects in oxidative phosphorylation. Methods *46*, 281-287.

Cavdar Koc, E., Ranasinghe, A., Burkhart, W., Blackburn, K., Koc, H., Moseley, A., and Spremulli, L.L. (2001). A new face on apoptosis: death-associated protein 3 and PDCD9 are mitochondrial ribosomal proteins. FEBS Lett *492*, 166-170.

Chen, H., Detmer, S.A., Ewald, A.J., Griffin, E.E., Fraser, S.E., and Chan, D.C. (2003). Mitofusins Mfn1 and Mfn2 coordinately regulate mitochondrial fusion and are essential for embryonic development. J Cell Biol *160*, 189-200.

Cheung, E.C., Joza, N., Steenaart, N.A., McClellan, K.A., Neuspiel, M., McNamara, S., MacLaurin, J.G., Rippstein, P., Park, D.S., Shore, G.C., McBride, H.M., Penninger, J.M., and Slack, R.S. (2006). Dissociating the dual roles of apoptosis-inducing factor in maintaining mitochondrial structure and apoptosis. Embo J *25*, 4061-4073.

Flores-Perez, U., Sauret-Gueto, S., Gas, E., Jarvis, P., and Rodriguez-Concepcion, M. (2008). A mutant impaired in the production of plastome-encoded proteins uncovers a mechanism for the homeostasis of isoprenoid biosynthetic enzymes in Arabidopsis plastids. Plant Cell *20*, 1303-1315.

Gordon, J. (1970). Regulation of the in vivo synthesis of the polypeptide chain elongation factors in Escherichia coli. Biochemistry *9*, 912-917.

Gray, M.W., Burger, G., and Lang, B.F. (2001). The origin and early evolution of mitochondria. Genome Biol *2*, REVIEWS1018.

Hofhaus, G., Shakeley, R.M., and Attardi, G. (1996). Use of polarography to detect respiration defects in cell cultures. Methods Enzymol *264*, 476-483.

Janssen, A.J., Smeitink, J.A., and van den Heuvel, L.P. (2003). Some practical aspects of providing a diagnostic service for respiratory chain defects. Ann Clin Biochem *40*, 3-8.

Janssen, A.J., Trijbels, F.J., Sengers, R.C., Smeitink, J.A., van den Heuvel, L.P., Wintjes, L.T., Stoltenborg-Hogenkamp, B.J., and Rodenburg, R.J. (2007). Spectrophotometric assay for complex I of the respiratory chain in tissue samples and cultured fibroblasts. Clin Chem *53*, 729-734.

Karbstein, K. (2007). Role of GTPases in ribosome assembly. Biopolymers *87*, 1-11.

Kim do, J., Jang, J.Y., Yoon, H.J., and Suh, S.W. (2008). Crystal structure of YlqF, a circularly permuted GTPase: implications for its GTPase activation in 50 S ribosomal subunit assembly. Proteins *72*, 1363-1370.

Koc, E.C., Burkhart, W., Blackburn, K., Moyer, M.B., Schlatzer, D.M., Moseley, A., and Spremulli, L.L. (2001). The large subunit of the mammalian mitochondrial ribosome. Analysis of the complement of ribosomal proteins present. J Biol Chem *276*, 43958-43969.

Lazarov, A., and Cooperstein, S.Y. (1951). Studies on the isolated islet tissue of fish. I. The cytochrome oxidase and succinic dehydrogenase contents of normal toadfish (Opsonus tau). Biol Bull *100*, 191-198.

Leipe, D.D., Wolf, Y.I., Koonin, E.V., and Aravind, L. (2002). Classification and evolution of P-loop GTPases and related ATPases. J Mol Biol *317*, 41-72.

Lietzke, R., and Nierhaus, K.H. (1988). Total reconstitution of 70S ribosomes from Escherichia coli. Methods Enzymol *164*, 278-283.

Loh, P.C., Morimoto, T., Matsuo, Y., Oshima, T., and Ogasawara, N. (2007). The GTP-binding protein YqeH participates in biogenesis of the 30S ribosome subunit in Bacillus subtilis. Genes Genet Syst *82*, 281-289.

Nierhaus, K. (1990). Reconstitution of ribosomes. In Ribosomes and protein synthesis A practical approach. G. Spedding, ed, 161-189.

Nierhaus, K.H. (1991). The assembly of prokaryotic ribosomes. Biochimie *73*, 739-755.
O'Brien, T.W. (2002). Evolution of a protein-rich mitochondrial ribosome: implications for human genetic disease. Gene *286*, 73-79.

Parihar, M.S., Parihar, A., Chen, Z., Nazarewicz, R., and Ghafourifar, P. (2008). mAtNOS1 regulates mitochondrial functions and apoptosis of human neuroblastoma cells. Biochim Biophys Acta *1780*, 921-926.

Qin, Y., Polacek, N., Vesper, O., Staub, E., Einfeldt, E., Wilson, D.N., and Nierhaus, K.H. (2006). The highly conserved LepA is a ribosomal elongation factor that back-translocates the ribosome. Cell *127*, 721-733.

Red-Horse, K., Zhou, Y., Genbacev, O., Prakobphol, A., Foulk, R., McMaster, M., and Fisher, S.J. (2004). Trophoblast differentiation during embryo implantation and formation of the maternal-fetal interface. J Clin Invest *114*, 744-754.

Sharpe, J., Ahlgren, U., Perry, P., Hill, B., Ross, A., Hecksher-Sorensen, J., Baldock, R., and Davidson, D. (2002). Optical projection tomography as a tool for 3D microscopy and gene expression studies. Science *296*, 541-545.

Smeitink, J., Sengers, R., Trijbels, F., and van den Heuvel, L. (2001). Human NADH:ubiquinone oxidoreductase. J Bioenerg Biomembr *33*, 259-266.

Srere, P. (1969). Citrate synthase, EC 4.1.3.7, citrate oxaloacetate lyase (CoA-acetylating). Methods Enzymol. *13*, 3-11.

Tang, T., Zheng, B., Chen, S.H., Murphy, A.N., Kudlicka, K., Zhou, H., and Farquhar, M.G. (2009). hNOA1 interacts with complex I and DAP3 and regulates mitochondrial respiration and apoptosis. J Biol Chem *284*, 5414-5424.

Uicker, W.C., Schaefer, L., Koenigsknecht, M., and Britton, R.A. (2007). The essential GTPase YqeH is required for proper ribosome assembly in Bacillus subtilis. J Bacteriol *189*, 2926-2929.

Vardi, A., Bidle, K.D., Kwityn, C., Hirsh, D.J., Thompson, S.M., Callow, J.A., Falkowski, P., and Bowler, C. (2008). A diatom gene regulating nitric-oxide signaling and susceptibility to diatom-derived aldehydes. Curr Biol *18*, 895-899.

Vortkamp, A., Lee, K., Lanske, B., Segre, G.V., Kronenberg, H.M., and Tabin, C.J. (1996). Regulation of rate of cartilage differentiation by Indian hedgehog and PTH-related protein. Science *273*, 613-622.

Wakabayashi, J., Zhang, Z., Wakabayashi, N., Tamura, Y., Fukaya, M., Kensler, T.W., Iijima, M., and Sesaki, H. (2009). The dynamin-related GTPase Drp1 is required for embryonic and brain development in mice. J Cell Biol *186*, 805-816.

Zemojtel, T., Frohlich, A., Palmieri, M.C., Kolanczyk, M., Mikula, I., Wyrwicz, L.S., Wanker, E.E., Mundlos, S., Vingron, M., Martasek, P., and Durner, J. (2006a). Plant nitric oxide synthase: a never-ending story? Trends Plant Sci *11*, 524-525; author reply 526-528.

Zemojtel, T., Kolanczyk, M., Kossler, N., Stricker, S., Lurz, R., Mikula, I., Duchniewicz, M., Schuelke, M., Ghafourifar, P., Martasek, P., Vingron, M., and Mundlos, S. (2006b). Mammalian mitochondrial nitric oxide synthase: characterization of a novel candidate. FEBS Lett *580*, 455-462.

Zemojtel, T., Penzkofer, T., Dandekar, T., and Schultz, J. (2004). A novel conserved family of nitric oxide synthase? Trends Biochem Sci *29*, 224-226.

Acknowledgments

We want to thank Monika Osswald, Petra Schrade and Carola Dietrich for excellent technical assistance. We also thank Malgorzata Gasperowicz and James Cross for providing template vectors for placenta specific riboprobes. We also want to acknowledge Laurene Marchand for her contribution in establishing mitochondrial membrane potential assay.

M.K. and N.K. were supported by the Young Investigator Award from Children Tumour Fundation – New York, Grant 2007-01-038 and by Bundesministerium für Bildung und Forschung, Grant NF1-01GM0844.

This work was also supported by the Sixth Framework of the European Commission, EuroGrow project LSHM-CT-2007-037471.

M.P. was supported by a DAAD grant and H. Y. by an Alexander-von-Humboldt stipendium.

RNL was supported by the Biotechnology and Biological Sciences Research Council, grant number BB/F011520/1.

I.M. and P.M. are supported by grants from MSMT, grant numbers 1M 6837805002 and 0021620806; and grant GAUK 252021 102107.

M.S. was supported by the Deutsche Forschungsgemeinschaft, NeuroCure Exc 257 and is a member of the German network for mitochondrial disorders (mitoNET, 01GM0862), funded by the German ministry of education and research (BMBF).

Table 1.

Stage	litters	*Noa1*+/+	*Noa1*+/-	*Noa1*-/-	in total
E7.5	2	2 (10%)	13 (65%)	5 (25%)	20
E8.5	7	14 (25%)	32 (58%)	9 (16%)	55
E9.5	16	21 (17%)	80 (66%)	20 (17.0%)	121
E10.5	5	6 (17%)	22 (61%)	8 (22%)	36
E14.5	1	2 (33.3%)	4 (66.6%)	0	6
E15.5	6	16 (31%)	36 (69%)	0	52
E16.5	2	5 (33.3%)	10 (66.6%)	0	15
P1	5	9 (25%)	27 (75%)	0	36
P28	11	32 (38%)	52 (62%)	0	84

Table 1. Intercross of *Noa1+/-* mice - offspring genotype distribution.
Knock-out embryos could not be detected beyond E10.5 indicating mid-gestation lethality. Heterozygous animals were born in expected mendelian ratio. No overt lethality of heterozygotes was observed in postnatal period.

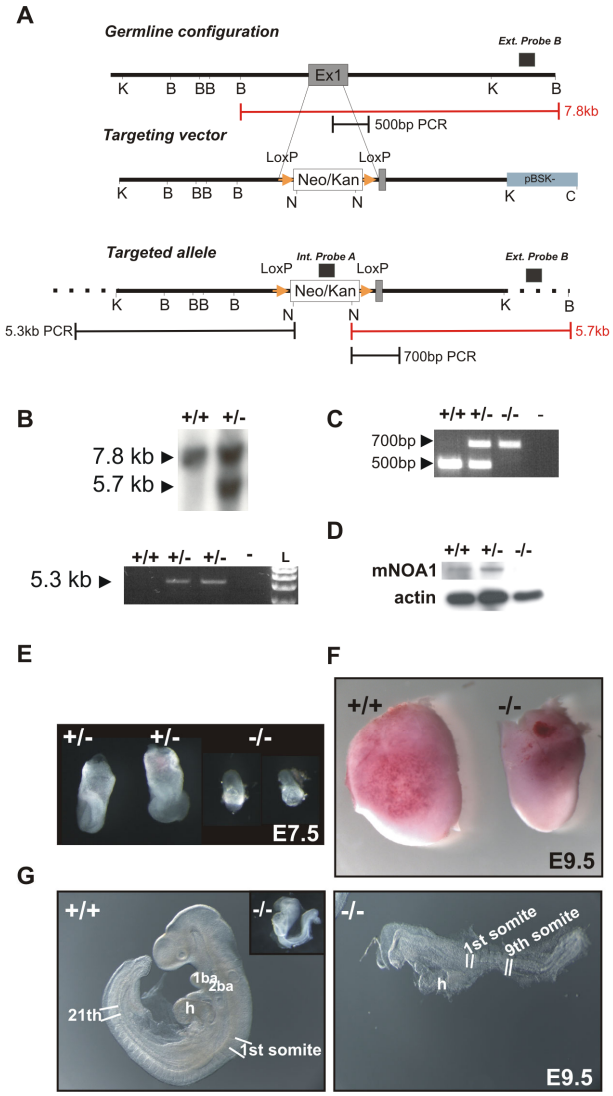

Figure 1. Generation of the *Noa1* knock-out mice.
(A) Strategy of *Noa1* gene targeting. The top bar indicates the enzymatic cleavage sites at the *Noa1* genomic locus (*BamH*I), K (*Kpn*I), N (*Not*I), C (*Cla*I). GTPase domain encoding Exon1 (dark grey segment) was targeted. Homologous recombination using thisconstruct (middle bar) resulted in a targeted allele (bottom bar) where a large part of exon1 was replaced by the *loxP* flanked, PGK-gb2 promoter driven, Neomycin/Kanamycin resistance cassette (white segment - Neo/Kan; yellow triangles - *loxP* sites). Insertion of the selection cassette introduced a *Not*I endonuclease recognition site enabling Southern blot based detection of homologous recombination with the internal and external probes (black boxes above the panels). Red rulers indicate expected *Bam*HI/*Not*I fragment sizes for the wt locus as well as the altered fragment size in the homologously targeted locus. Black rulers indicate lengths of the long range PCR products obtained from the wt and homologously targeted locus. (B) Southern-blot and long-range-PCR based detection of the homologous recombination, and (C) PCR based genotyping strategy. (D) Western blot analyses of E9.5 wt, *Noa+/-* and *Noa1-/-* embryo lysates with ß-actin as loading control. (E) Appearance of *Noa1* knock-out embryos at E7.5. (F) A comparison of the intact embryos at E9.5 is shown to illustrate the difference in size. (G) *Noa1* knock-out embryo development is arrested at pre-rotation stage (insert). E9.5 wt embryo displays 21 somites while NOA1 deficient littermate (magnified) reaches maximally 9-somites stage. See also Movie S1 and S2 available online.

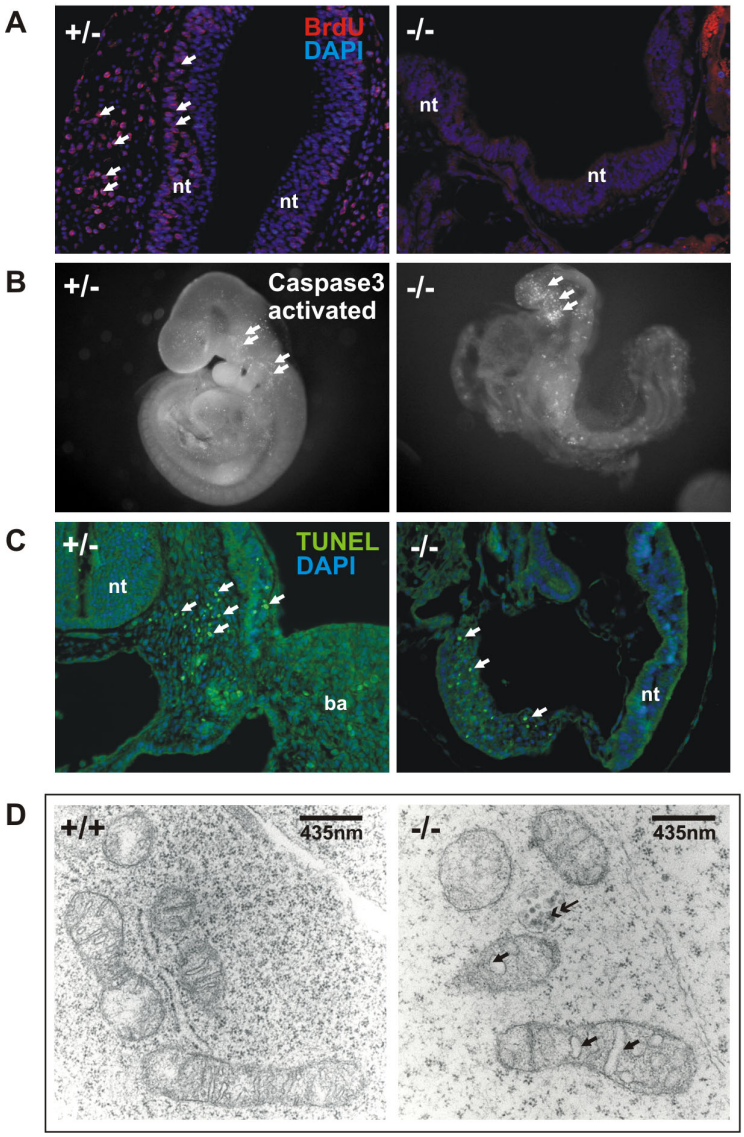

Figure 2. Phenotype of *Noa1* knock-out mice.

(A) BrdU in-vivo labeling reveals arrest of proliferation in the E9.5 *Noa-/-* embryos. (B, C) Apoptosis in the E9.5 *Noa1-/-* embryos visualized by anti activated caspase-3 immunolabeling in the whole mount preparations (B) and TUNEL staining on paraffin sections (C). Data are representative of at least 3 embryos analysed for each genotype. (D) Electron microscopic analysis of the *Noa1-/-* embryos. Many mitochondria show aberrant morphology characterized by swollen intracristal spaces (single-headed arrows). Some appear collapsed into electron dense, shrunken remnants (double-headed arrow). ER and other organelles appear normal in *Noa1-/-* embryos (data not shown). ba – branchial arche, h – heart, nt – neural tube.

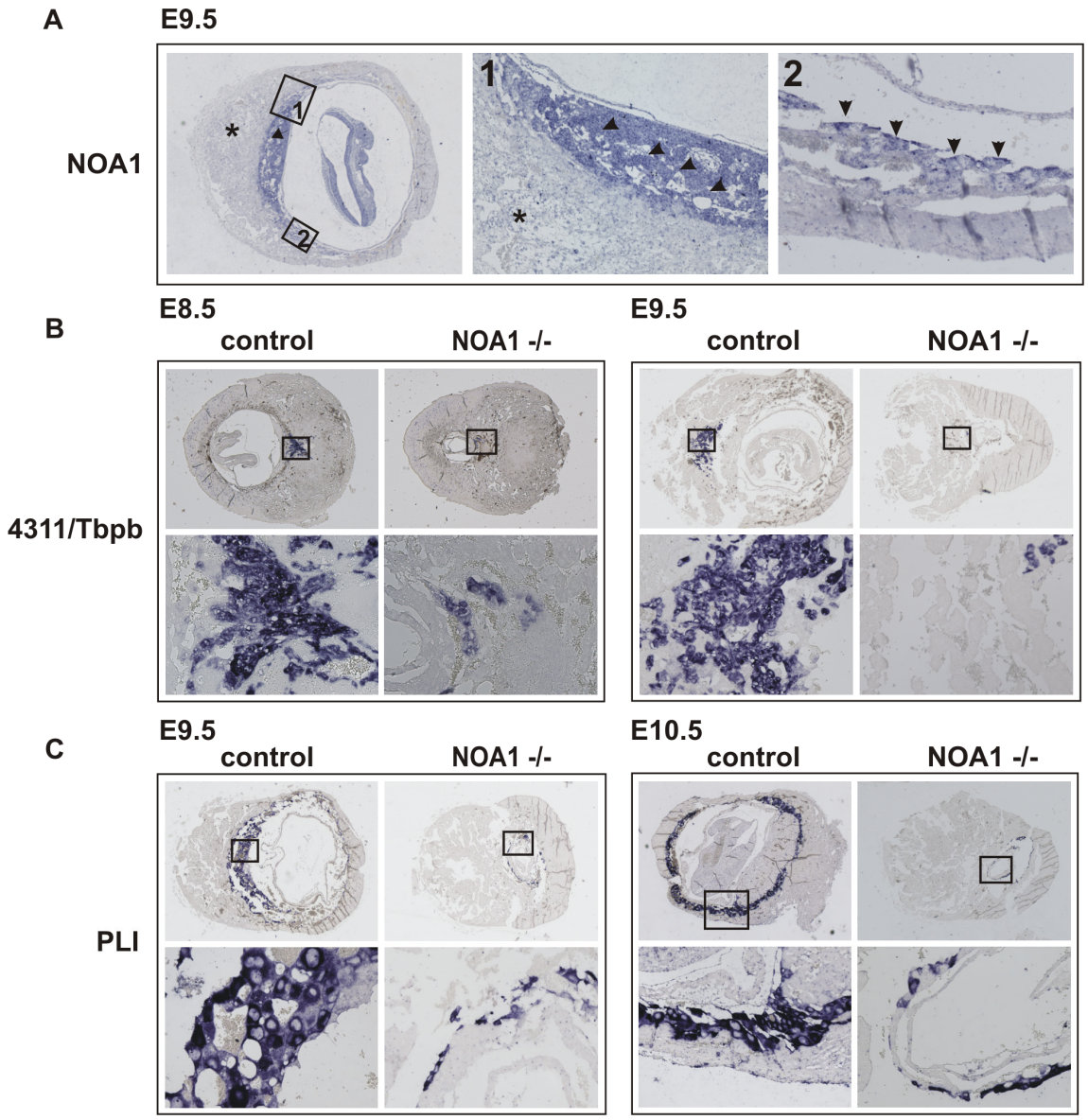

Figure 3. *Noa1* is indispensable for placental trophoblast development.

In-situ hybridization on the sections of E8.5, E9.5 and E10.5 wild-type and mutant littermate embryos at the implantation sites. Boxed areas in the upper panels are enlarged in lower panels. (A), *Noa1* expression is restricted to the placental trophoblast at E9.5 (arrow). Intense expression in the labyrinth and spongiotrophoblast (arrowheads - magnification 1) and in the trophoblast giant cells (arrows - magnification x2). *Noa1* expression could not be detected in the maternal part of the placenta (star) nor in the knock-out embryos (data not shown). (B), defect of the trophoblast progenitor cell differentiation in the *Noa1-/-* mice. 4311/Tbpb is expressed in the trophoblast progenitor cells which give rise to glycogen cells and secondary giant trophoblast cells. Diminished 4311/Tbpb expression in the E8.5, E9.5 ectoplacental cone. (C), defect of trophoblast giant cell differentiation in E9.5 and 10.5 *Noa1-/-* embryos visualized by diminished expression of placental lactogen 1 (PL1).

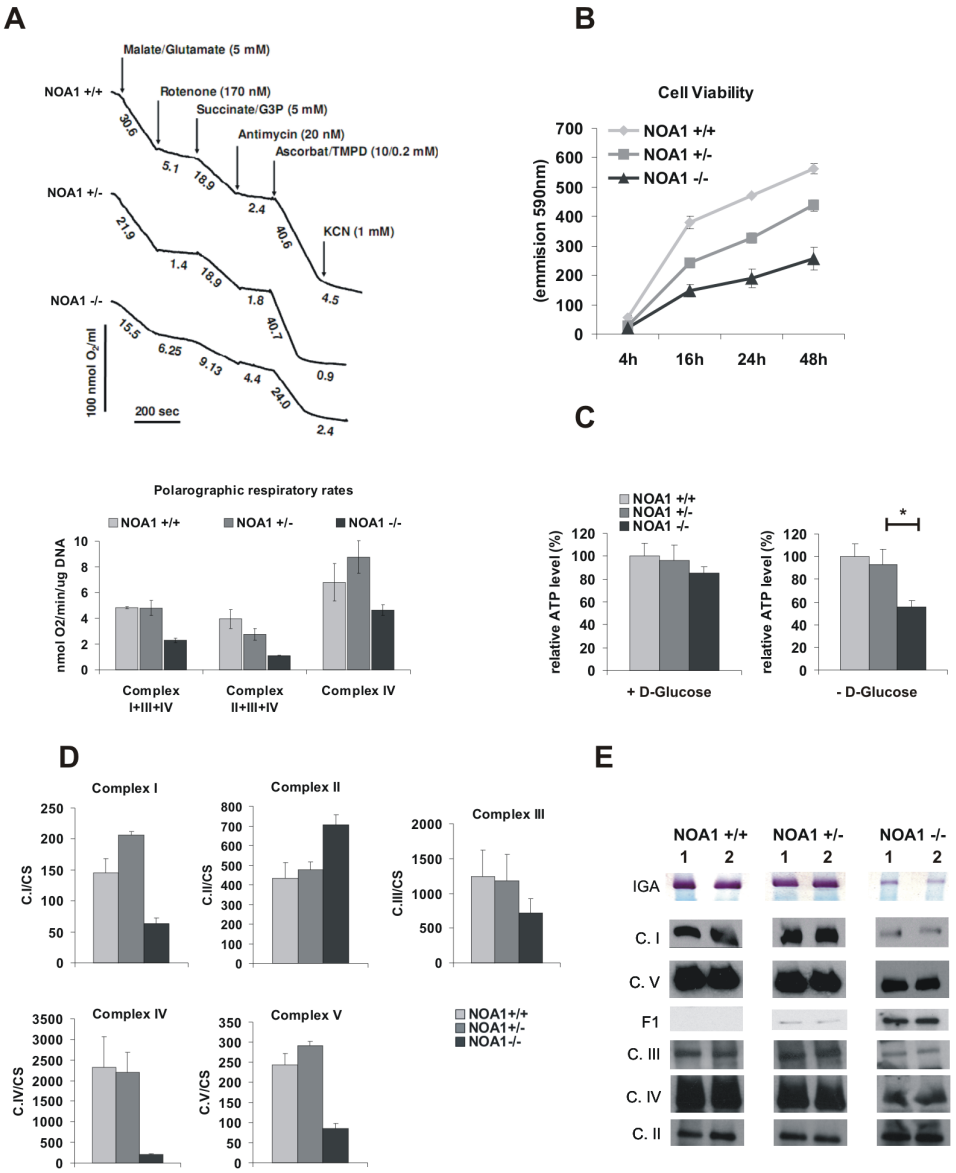

Figure 4. OXPHOS deficiency in *Noa1-/-* cells.
(A) Cells were permeabilized with digitonin and oxygen consumption was monitored polarographically in the presence of respiratory chain substrates and inhibitors. Note a marked decrease of the complex I, III and IV dependent oxygen consumption but not complex II dependent oxygen consumption. Results represent mean ± SD of three independent experiments. (B) Reduced viability of the NOA1 deficient cells determined with the AlamarBlue. (C) *Noa1-/-* cells show reduced ATP levels upon glucose deprivation. See also Supplemental Information, Figure S6 for genetic complementation data. (D) Reduced enzymatic activities of the mitochondrial complex I, III, IV and V in the knock-out cells. In contrast complex II activity was increased. The enzymatic assay values are shown standardized to citrate synthase E3 activity (CS). Results represent mean ± SD of three independent experiments. (E) (IGA) In-gel activity of complex-I is decreased in knock-out cells. Blue native electrophoresis (BN) showing reduction in quantities of the assembled complex I, III, IV and V and accumulation of the unassembled complex V intermediate (F1) in the homozygous *Noa1* mutant cells.

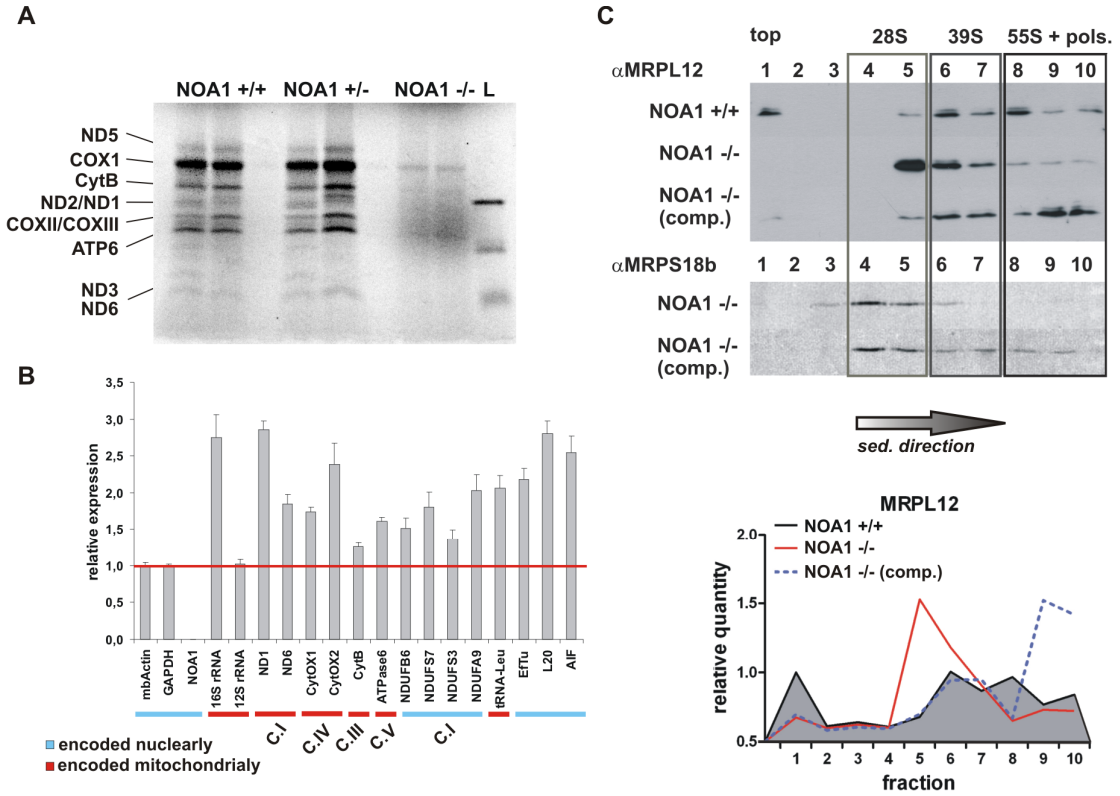

Figure 5. NOA1 deficiency impairs mitochondrial protein synthesis.

(A) [^{35}S]-methionine labelling of mitochondrial protein synthesis in primary embryonic fibroblasts reveals deficient translation in NOA1 knock-out cells. Concentrations of protein lysates were calculated by the BCA method and equal loading was confirmed by coomassie staining following exposure (not shown). (B) Real time PCR quantification of the mitochondrial gene transcript levels. RNA species encoded by mitochondrial (underlined red) and nuclear (underlined blue) DNA were quantified. Data were normalized against GAPDH and Actin expression. (C) Cell lysates were fractionated in the 10–30% (v:v) isokinetic sucrose gradients and analyzed by Western blots with antibodies against MRPL12 (39S mitoribosomal subunit) or MRPS18b (28S mitoribosomal subunit). Representative blots were analyzed densitometrically (lower panel). See also Figure S4 for genetic complementation data. (comp. – knock-out cells with retroviral complementation of NOA1 expression).

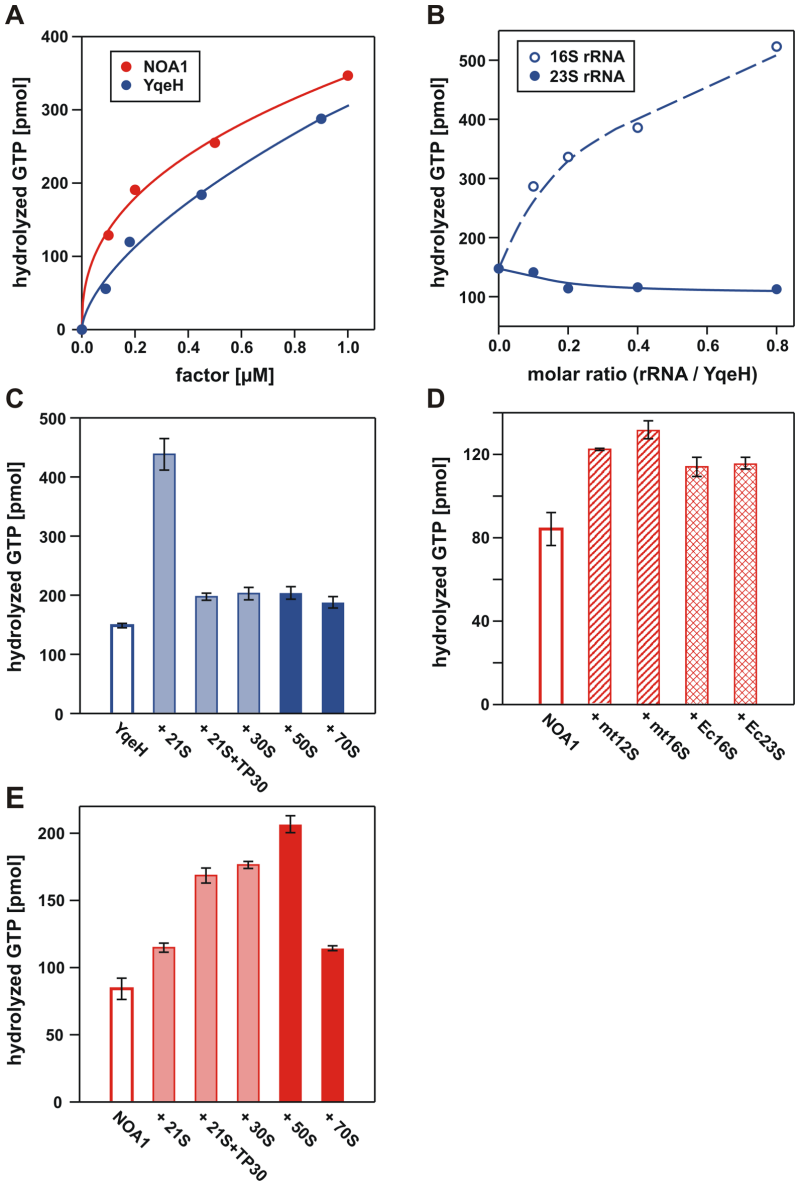

Figure 6. GTPase activities of NOA1 and YqeH are differently stimulated by ribosomal components from *E. coli*.

(A) Intrinsic GTPase activities of NOA1 and YqeH at 30°C. (B) Specific stimulation of YqeH GTPase activity by *E. coli* 16S rRNA at 30°C. (C) Specific stimulation of YqeH GTPase by equimolar amounts of *E. coli* 30S precursors (21S) in comparison to total reconstituted 30S subunits (21S+TP30), ribosomal subunits (30S, 50S) and 70S ribosomes at 20°C. (D) Stimulation of NOA1 GTPase by equimolar amounts of mitochondrial rRNA (mt12S, mt16S) and *E. coli* rRNA (Ec16S, Ec23S) at 20°C. (E) Stimulation of NOA1 GTPase by equimolar amounts of *E. coli* 30S precursors before (21S) and after total reconstitution of 30S particles (21S+TP30), ribosomal subunits (30S, 50S) and 70S ribosomes at 20°C.

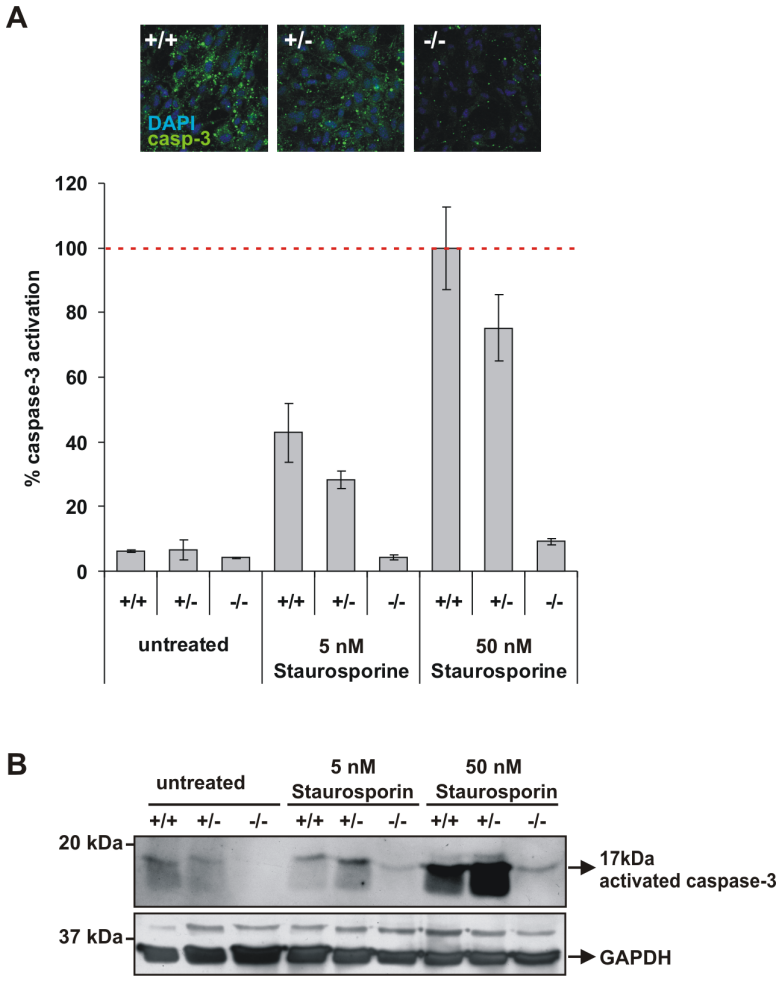

Figure 7. *Noa1*-deficient cells are resistant to staurosporine-induced apoptosis

Embryonic fibroblasts were cultured on cover slips in presence of increasing concentrations of staurosporine. Apoptosis was monitored by measuring activation of the caspase-3. (A) Caspase-3 positive area was quantified using ImageJ software and corrected for the cell number. Representative microscopic pictures are shown (data represent mean of at least 10 evaluated images with S.E.M as error bars) (B) Western blot with anti-activated Caspase-3 antibodies. Blots were striped and probed with the antibody against GAPDH for loading control.

Competing Financial Interests

The authors declare no competing financial interests.